blood advances

American Society of Hematology
2021 L Street NW, Suite 900,
Washington, DC 20036
Phone: 202-776-0544 | Fax 202-776-0545
bloodadvances@hematology.org

# Dual role of signaling pathways in myeloma requires cell-type specific targeting of ligand-receptor interactions.

Tracking no: ADV-2023-011463R1

Pablo Hernandez-Lopez (Dana-Farber Cancer Institute, United States) Tushara Vijaykumar (Dana-Farber Cancer Institute, United States) Praveen Anand (Harvard Medical School, United States) Daniel Auclair (MMRF, United States) Julia Frede (Harvard Medical School, United States) Birgit Knoechel (Harvard Medical School, United States) Jens Lohr (Harvard Medical School, United States)

**Abstract:**
Although most patients with multiple myeloma respond to treatment initially, therapy resistance develops almost invariably and only a subset of patients show durable responses to immunomodulatory (IMiD) therapies. While the immune microenvironment has been extensively studied in myeloma patients, its composition is currently not used as prognostic markers in clinical routine. We hypothesized that the outcome of immune signaling pathway engagement can be highly variable, depending on which two cellular populations participate in this interaction. This would have important prognostic and therapeutic implications, suggesting that it is crucial for immune pathways to be targeted in a specific cellular context. To test this hypothesis, we investigated a cohort of 27 patients with newly diagnosed multiple myeloma. We examined the complex regulatory networks within the immune compartment and their impact on disease progression. Analysis of immune cell composition and expression profiles revealed significant differences in the B cell compartment associated with treatment response. Transcriptional states in patients with short time to progression demonstrated an enrichment of pathways promoting B cell differentiation and inflammatory responses, which may indicate immune dysfunction. Importantly, the analysis of molecular interactions within the immune microenvironment highlights the dual role of signaling pathways, which can either be associated with good or poor prognosis depending on the cell types involved. Our findings therefore argue that therapeutic strategies targeting ligand-receptor interactions should take into consideration the composition of the microenvironment and the specific cell types involved in molecular interactions.

**Conflict of interest:** No COI declared

**COI notes:**

**Preprint server:** No;

**Author contributions and disclosures:** J.F., P.A., T.V. and P.A. designed and performed data analysis. J.F., B.K. and J.G.L. designed experiments, provided project leadership, supervised the analysis and wrote the manuscript. All authors discussed the results and reviewed the manuscript.

**Non-author contributions and disclosures:** No;

**Agreement to Share Publication-Related Data and Data Sharing Statement:** The sequencing data used in this study have been deposited in the Gene Expression Omnibus (GEO) database and can be accessed under accession number GSE263702.

**Clinical trial registration information (if any):**

**ARTICLE TITLE:**

# Dual role of signaling pathways in myeloma requires cell-type specific targeting of ligand-receptor interactions.

- short title for the running head: **Dual interactions require cell-specific targeting.**
- word counts for text and abstract, figure/table count and reference count:
  - Text: 4000/4000
  - Abstract: 238/250
  - Figures: 5/7
  - References: 50/100

Pablo Hernandez Lopez[1], Tushara Vijaykumar[1], Praveen Anand[1,2,3], Daniel Auclair[4], Julia Frede[1,2,3,6,*], Birgit Knoechel[2,3,5,6,*], Jens G. Lohr[1,2,3,6,*]

[1]Department of Medical Oncology, Jerome Lipper Multiple Myeloma Center, Dana Farber Cancer Institute, Boston, MA, USA

[2]Harvard Medical School, Boston, MA, USA

[3]Broad Institute of MIT and Harvard, Cambridge, MA, USA

[4]Multiple Myeloma Research Foundation, Norwalk, CT, USA

[5]Department of Pediatric Oncology, Dana-Farber Cancer Institute, Boston, MA, USA

[6]These authors jointly supervised this work.

[*]Correspondence: julia_frede@dfci.harvard.edu, jensg_lohr@dfci.harvard.edu, birgit_knoechel@dfci.harvard.edu

The sequencing data used in this study have been deposited in the Gene Expression Omnibus (GEO) database and can be accessed under accession number GSE263702.

**Abstract (238/250 words)**

**Although most patients with multiple myeloma respond to treatment initially, therapy resistance develops almost invariably and only a subset of patients show durable responses to immunomodulatory (IMiD) therapies. While the immune microenvironment has been extensively studied in myeloma patients, its composition is currently not used as prognostic markers in clinical routine. We hypothesized that the outcome of immune signaling pathway engagement can be highly variable, depending on which two cellular populations participate in this interaction. This would have important prognostic and therapeutic implications, suggesting that it is crucial for immune pathways to be targeted in a specific cellular context.**

**To test this hypothesis, we investigated a cohort of 25 patients with newly diagnosed multiple myeloma. We examined the complex regulatory networks within the immune compartment and their impact on disease progression. Analysis of immune cell composition and expression profiles revealed significant differences in the B cell compartment associated with treatment response. Transcriptional states in patients with short time to progression demonstrated an enrichment of pathways promoting B cell differentiation and inflammatory responses, which may indicate immune dysfunction. Importantly, the analysis of molecular interactions within the immune microenvironment highlights the dual role of signaling pathways, which can either be associated with good or poor prognosis depending on the cell types involved. Our findings therefore argue that therapeutic strategies targeting ligand-receptor interactions should take into consideration the composition of the microenvironment and the specific cell types involved in molecular interactions.**

**Key Points**

- **An identical molecular interaction can confer either good or poor prognosis, depending on the cell types involved.**
- **Therapeutic strategies targeting ligand-receptor interactions should take into consideration the specific cell types involved.**

## Introduction

Tumors embody complex ecosystems, and variability in the composition of immune components and expression are linked to distinct cancer subtypes and treatment results. Despite initial therapeutic responses in multiple myeloma (MM) patients, treatment resistance often leads to eventual relapse. IMiDs—thalidomide and its derivatives lenalidomide and pomalidomide—have become pervasive in myeloma treatment[1-3] due to their diverse mechanisms, including anti-angiogenic, cytotoxic, and immunomodulatory properties.[4,5] However, despite their efficacy[6-8], IMiDs do not yield lasting responses in all patients and resistance is common. Beyond IMiDs, other immunotherapies have shown success in myeloma treatment, underlining the critical role of the bone marrow immune microenvironment[9]. Nevertheless, persistent immunotherapeutic responses are observed only in a subset of patients. Therefore, to enhance patient outcomes, we need a better understanding of the immune microenvironment, the factors determining response to therapies, and predictive markers for response and disease progression.

The bone marrow immune microenvironment is composed of a large variety of immune cells, including CD4+ and CD8+ T cells, regulatory T cells (Tregs), myeloid-derived suppressor cells (MDSCs), natural killer (NK) cells, and diverse B cell subsets. Past research indicates considerable shifts within the MM bone marrow microenvironment, such as cytokine secretion and compositional changes[10]. MM cells have been shown to induce immunosuppression via elevated numbers of Tregs, MDSCs, non-traditional monocytes, and alterations in T and NK cell populations[10]. Yet, the implications of changes in the B cell compartment on the antitumor immune response or immune evasion remain undetermined.

Compositional shifts in the cellular architecture of the bone marrow play a vital role in the initiation and progression of MM[11,12]. These shifts support pro-inflammatory states and immunosuppression, thereby enabling immune evasion and disease progression through

intricate interactions between immune cells, stromal elements, and malignant plasma cells[11-13]. In this study, we aim to better comprehend the complex interregulation within the immune compartment in patients with newly diagnosed (ND) MM, identify the key participants and their influence on treatment resistance and disease progression.

Importantly, the heterogeneity of immune cell composition among patients has potential as a critical biomarker, carrying prognostic value and influencing therapeutic strategies[10]. Here we correlated alterations in cell type composition and expression profiles with therapy response. Our findings delineate the transcriptional and compositional shifts in the bone marrow immune microenvironment during disease progression, highlighting mechanisms for antitumor immune response and immune evasion. We examined cell-cell interactions to identify the factors that condition the fate and functionality of immune cell subsets in the bone marrow. Interestingly, our studies of molecular interactions within immune compartments revealed that the same signaling pathway can convey either positive or negative prognosis, contingent on the specific cell types interacting. We propose a model underscoring the dual role of cell-cell interactions, where the same interaction can generate both favorable and adverse outcomes depending on the involved cell types and signal directionality. Our studies support the notion that therapies aimed at targeting ligand-receptor interactions should consider the microenvironment's composition and the particular cell types partaking in molecular interactions to block harmful signals while preserving beneficial ones.

## Methods

### Patient samples

Cryopreserved CD138- bone marrow samples from 25 treatment-naïve newly-diagnosed myeloma (NDMM) patients were analyzed in this study (Supplementary Table 1). Bone marrow from normal donors was obtained from AllCells.

**Cell sorting**

Cells were stained with antibodies against CD45 FITC (HI30, eBioscience, 1:100), CD3 PerCP-Cy5.5 (OKT3, eBioscience, 1:100), CD14 APC-Cy7 (MoP9, BD Biosciences, 1:100), CD19 PE (HIB19, BioLegend, 1:100). Dead cells were excluded with DAPI (1µg/mL, Sigma-Aldrich). A hundred cells per well were sorted into 96-well plates using a Sony SH800 sorter. Percentages of positive cells were calculated using FlowJo software v10. Statistical analysis was performed using GraphPad software.

**Low-input RNA-Seq library preparation**

Low-input RNA-Sequencing libraries were prepared using the SmartSeq2 protocol[14] as described previously[31]. Pooled libraries were paired-end sequenced using a 75 cycle kit on a NextSeq 500 (Illumina) with an average sequencing depth of 1 million reads per sample.

**Processing of RNA-Seq data**

Sequencing reads were trimmed using trimmomatic and aligned to the human genome (version hg19) using STAR aligner with following parameters '-- twopassMode Basic –alignIntronMax 100000 --alignMatesGapMax 100000 --alignSJDBoverhangMin 10 --alignSJstitchMismatchNmax 5 -1 5 5'[15,16]. HTSeq[17] and RSEM[18] were used to obtain raw counts and normalized TPM values from the aligned BAM files.

**Quality control and processing of RNA-Seq data**

To remove low-quality samples from our dataset, we used the following cutoffs: for library size, detected genes, and percentage counts mapping to ribosomal genes 4 median-absolute-deviations; for mitochondrial genes 2 median-absolute-deviations. Dimensionality reduction and clustering of high-quality samples were performed using the scater[19] and scran packages[20]. Signaling pathway activity was inferred using the PROGENy package[20,21].

**Deconvolution analysis**

Cell type composition from bulk expression profiles was inferred using Cibersort[22]. Cibersort was run using default settings providing the normalized expression matrix as input. Statistical analysis was performed using GraphPad software.

**Inference of cell-cell interactions**

Cell-cell interactions were inferred based on ligand-receptor co-expression using the CellphoneDB package (v2.0) with default settings[23]. Analysis of cell-cell interactions was performed separately for patients with good (TTPhigh) or poor (TTPlow) prognosis. Interactions were considered specific to one prognosis ("prognostic interactions") if they were detected as significant ($p$-value$<0.05$) in one condition, but not the other ($p$-value$\geq 0.05$).

**Validation of gene expression**

We validated expression of the interacting molecules in the relevant cell types using scRNA-seq data from the Human Protein Atlas and Bloodspot (Blueprint dataset)[24,25].

**Validation cohorts**

Published single-cell RNA-Sequencing data from patients treated with IMiDs[26-28] or with non-IMiD-based treatments[27,29] were obtained for validation. Data were pre-processed using Cell Ranger Ranger 6.1.0[30] and Seurat V4[31]. Celltype annotation was performed using azimuth

(https://app.azimuth.hubmapconsortium.org/app/azimuth-bone-marrow) and the human bone marrow dataset as a reference. CITE-Seq data were obtained from GSE210079[29].

Informed consent has been obtained from all patients in this study.

## Results

### Heterogeneous bone marrow immune cell composition in treatment-naive MM patients

We hypothesized that the outcome of activating an immune signaling pathway can vary based on the cell types involved in the interaction. Since immune cell composition is heterogeneous in MM[10], we first sought to identify those cell populations with the greatest difference in abundance between patients with better or worse outcome, postulating that these would be most likely to engage in interactions that are relevant for patient outcome.

To define the composition of the bone marrow immune compartment in treatment-naive patients with multiple myeloma, we investigated bone marrow aspirates from a cohort of 25 NDMM patients. Median time to progression in this cohort was 28 months and 76% of patients received first line treatment with an IMiD (Fig. 1a,b). We performed fluorescence activated cell sorting (FACS) to enrich for distinct immune cell populations in the bone marrow, CD45+CD3+ cells to enrich for T cells, CD45+CD19+ to enrich for B cells, CD45+CD14+ to enrich for classical monocytes and CD45+CD3-CD19-CD14- (CD45+Lin-) to enrich for other immune cell subtypes (Fig. 1c, Supplementary Fig. 1a). Consistent with previous studies[10], patient bone marrow immune cell compositions demonstrated considerable variability, with CD3+ cells accounting for 1-77% of CD45+ immune cells in the bone marrow (mean 30%, range 1-77%), CD19+ cells accounting for 0-22% (mean 6%, range 0-22%), CD14+ for 3-56% (mean 16%, range 3-57%) and CD45+Lin- for 7-85% (mean 49%, range 7-85%) (Fig. 1d).

To assess whether bone marrow immune cell composition correlated with time to progression (TTP), we divided the patient cohort by median time to progression into TTPlow patients

displaying early relapse and TTPhigh patients showing late relapse (Fig. 1e). We compared proportions of immune cell subsets between conditions and observed that patients with early relapse displayed higher proportions of CD14+ cells (p=0.0295 by unpaired t-test), arguing that presence of monocytes is negatively correlated with time to progression (Fig. 1f,g). As we observed a high degree of variability between patients, we also compared the 25th/75th percentiles, and observed that patients with very late relapse showed a higher proportion of CD3+ cells and CD19+ cells than patients with very early relapse, indicating that greater numbers of T and B lymphocytes have a favorable impact on prognosis (p=0.03 and p=0.005 by unpaired t-test, respectively; Supplementary Fig. 1b-d).

To define the cell type composition and expression profiles of different immune cell subtypes in the bone marrow in greater detail, we next performed FACS sorting and low-input RNA-sequencing using the Smartseq2 technology (Fig. 1h). To enhance the detection of genes, improve data quality, and enhance statistical power, we implemented a strategy of examining 'minipools' of cells. After quality control filtering, we performed clustering and visualization by t-distributed stochastic neighbor embedding (tsne) as an initial assessment of heterogeneity (Fig. 1i, Supplementary Fig. 2a,b). Clustering was determined by sorted surface marker, but not by individual or prognostic condition (Fig. 1i, Supplementary Fig. 2c-g). We next assessed expression of lineage defining marker genes, including CD3D for T cells, CD19 for B cells and CD14 for monocytes (Supplementary Fig. 2e-g). We confirmed this by assessing expression of canonical marker genes for different immune cell types (Fig. 1j).

**Differential enrichment of B-cell subsets associated with prognosis**

To define in greater detail which cell types and maturation states were enriched in the various immune compartments, we assessed expression of gene signatures (Fig. 2a). We recovered expression of the gene signatures for pre-B cells, naive B cells, transitional B cells, memory B

cells and plasma cells in the CD19+ compartment, indicating that this compartment contains a mixture of B cell subtypes. Similarly, in the CD14+ compartment, we detected expression of marker genes for monocytes, dendritic cells and macrophages. In the CD3+ compartment, we detected expression of gene signatures related to various CD8+ and CD4+ T cells subtypes and to a lesser degree NK cells, presumably as both cell types share expression of certain genes, while the CD45+CD3-CD19-CD14- compartment was enriched in NK cells and dendritic cells.

To comprehensively assess the relative abundance of different cell types in the bone marrow, we performed deconvolution of cell types using cibersort[22] (Fig. 2b-f). Consistent with our signature-based analysis, we identified naïve and memory B cells as well as plasma cells in the CD19+ subset, CD4+ and CD8+ T cells in the CD3+ compartment, activated and resting NK cells as well as dendritic cells and presumably non-classical monocytes in the CD45posTN subset, and mostly monocytes in the CD14+ subset.

We then assessed how cell type composition in newly diagnosed myeloma patients differed from normal donors (Supplementary Fig. 3a-c). Memory B cells were significantly enriched in myeloma patients (p=0.0106 by two-tailed T-test, mean=50.3% of CD19+ cells in MM, range 0-83% vs 8%, range 0-23% in ND), as were T follicular helper (Tfh) cells (p=0.046, mean=7.5% of CD3+ cells, range=1.9-18.9% in MM vs mean=2.7%, range=0-6.7% in ND) (Supplementary Fig. 3d). Tfh cells are commonly located in secondary lymphoid organs, including the tonsil, spleen, and lymph nodes, but they have been described in the bone marrow in hematological diseases[32,33]. Interestingly, Tfh cells may help naive B cells to differentiate into memory B cells[34], which is consistent with our observation of differentiation towards a memory-B-cell phenotype in MM. Conversely, we observed a decreased abundance of naive B cells (p=0.0436 by t-test, mean= 32.7% of CD19+ cells, range=0-77% in MM vs mean 62.3%, range=52-71% in

ND) and M2 macrophages in MM (p=0.0017 by t-test, mean= 1.4%, range 0-3.8% in MM vs mean= 12.1%, range = 0.7-19.7% in ND).

To determine which of those cell types correlate with response to therapy, we then compared cell type abundance in patients with early relapse vs late relapse (Fig. 2g-l). Interestingly, the proportion of naive B cells was higher in patients with late relapse (p= 0.047 by t-test, mean=47.5%, range=7-77% in TTPhigh patients vs mean=21.2, range 2-70% in TTPlow patients; Fig. 2i), while the proportion of memory B cells was decreased in patients with late relapse compared to those with early relapse (p=0.0488 by t-test, mean= 34.6%, range=4-80% in TTPhigh patients vs mean=62.6%, range=0-87% in TTPlow patients; Fig. 2j). The ratio of naive:memory B cells was significantly higher in TTPhigh patients (p= 0.041 by t-test, Fig. 2k), indicating that there is a shift from naive to memory B cells in patients with early relapse and that having less differentiated B cells is correlated with good prognosis. We also observed an increased abundance of activated NK cells in patients with late relapse (p=0.0435 by t-test, mean=10.4%, range=3-23% in TTPhigh vs mean=1.3%, range=0-4% in TTPlow patients; Fig. 2l). In line with previous studies[35], these data suggested that an immunocompetent microenvironment with adequate B cell capacity is an important factor for the efficacy of IMiD-based therapy.

To define the functional effect of compositional changes in the bone marrow microenvironment between patients with short and long time to progression, we assessed gene expression signatures. We observed increased expression of a gene set associated with naive B cells in patients with late relapse (TTP high; p=0.027; Fig. 2m), consistent with our previous observations. We confirmed this association in an independent dataset (GSE161801)[27] consisting of 9 relapsed/refractory myeloma patients receiving IMiD-based treatments (p<2.2e-

16 by test, Supplementary Fig. 4a). Furthermore, the expression score for naïve B cells correlated with time to progression (R=0.56, p=0.036).

When assessing expression of marker genes for either naive or memory B cells, we detected enrichment in patients with late and early relapse, respectively (Fig. 2n). Other marker genes in the CD19+ immune compartment in patients with late relapse included the transcription factor *HELIOS* (*IKZF2*), while in TTPlow patients we detected expression of interferon-response genes, suggesting that the B cell compartment might receive divergent signals from the environment (Fig. 2o). We therefore analyzed cell signaling pathways (Fig. 2p) using PROGENy[21]. Consistent with greater expression of interferon-responsive genes, we predicted greater activation of JAK-STAT signaling in patients with poor prognosis, as well as greater activity in EGFR and VEGF signaling pathways. In contrast, patients with good prognosis showed greater activation of the TNFa and MAPK signaling pathways.

**Prognostic impact of cell-cell interactions depends on involved cell types**

Our data and prior studies indicate that the bone marrow microenvironment in MM exhibits dysregulation in receptor signaling[36], cytokine expression[27,36] and numerical alterations in immune cell subsets[10,37,38]. Surface interactions are the main drivers of intracellular signaling and therefore control the fate and function of cells. To define the underlying causes that are conditioning the fate and functions of immune cell subsets in the bone marrow, we therefore investigated cell-cell interactions using CellPhoneDB[23].

We predicted cell-cell interactions between and within the immune cell compartments in both prognostic conditions (Fig. 3a,b). We found that the distribution of interactions of the different immune cell compartments was similar in both conditions, with slightly more interactions detected in the CD3+ compartment and less in the CD19+ compartment in TTPhigh patients

(32% vs 29% of interactions for CD3+ and 17% vs 20% of interactions for CD19+ in TTPhigh vs TTPlow). As we had identified significant compositional changes in the B cell compartment, we next went on to assess cell interactions with a focus on CD19+ cells (Fig. 3c,d). We identified a total of 438 inferred interactions in TTPhigh and 523 interactions in TTPlow patients (Supplementary Tables 2,3). We observed that B cells interact most with CD3+ cells and least with other CD19+ cells. In TTPlow patients we observed more interactions with CD14+ cells compared to TTPhigh patients (Fig. 3d). To assess the association of these cell-cell interactions with prognosis in greater detail, we next filtered the interactions that were significant ($p<0.05$) in one condition (TTP status), but not significant ($p\geq 0.05$) in the other (see Methods). These prognostic interactions accounted for 24% and 22% of total identified interactions in TTPhigh patients (107/438, 24%) and in TTPlow patients (113/523, 22%), respectively (Fig. 3e, Supplementary Tables 2-5).

Remarkably, we observed that some of these “prognostic” interactions were present in both conditions at the same time. These interactions took place between different cell types or the ligand/receptor expression was switched between the involved cell types (illustrated in Fig. 4a). These data suggest a model, in which the selectivity of these dual interactions is determined by the cellular partner (cellular partner selectivity) that the B cell interacts with. Thus, if the interacting receptor/ligand is expressed by cell type A, the interaction confers good prognosis, while the same interacting ligand/receptor expressed by cell type B confers poor prognosis. Alternatively, it is also conceivable that the B cell expresses both the receptor and the ligand, and the prognosis is determined by the directionality of the signal, i.e. the other cell type that expresses the ligand or the receptor. We referred to these interactions as “dual interactions”, to highlight their ambiguous role as the net effect on the prognosis is neither solely favorable nor unfavorable. We identified a total of sixty-four dual interactions (Supplementary Table 6) and assessed their distribution across the different interacting cell types within each prognostic

condition (Fig. 4b). We observed an enrichment of these interactions in CD45+TN and CD3+ cells in the TTPhigh group and in CD14+ and CD19+ cells in the TTPlow group.

To identify candidate interactions with therapeutic potential, we focused on molecules expressed at the cell surface as we hypothesized that these might represent potential therapeutic targets, being accessible at the cell surface and potentially targetable by immunotherapy/CAR-T cells. We identified a subset of 13 surface-restricted dual interactions that may serve as potential therapeutic targets (Fig. 4c). For example, we identified an interaction of IL15 and IL15RA among the dual interactions. When IL15 is expressed by the B cell and interacts with IL15RA on the CD3+ or CD45+TN cells, it confers a favorable prognosis. Trans-presented IL15 sensed by NK cells and T cells triggers immune activation and cytotoxicity[39-42]. However, in patients with short time to progression both the receptor IL15RA and the ligand IL15 are expressed by CD19+ cells and CD14+ cells, suggesting the possibility of bi-directional signaling (Fig. 4c). IL15 trans-presentation involving CD14+ cells has been reported to induce secretion of pro-inflammatory cytokines and chemoattractants, such as IL1, IL6, IL8, and TNF-α, and MCP-1[42-44]. Therefore, the same interaction can result in increased anti-tumor immunity or in the creation of a pro-inflammatory immunosuppressive microenvironment, depending on the cell types involved. We further validated expression of these molecules in the relevant interacting cell types using the Human Protein Atlas and Bloodspot (Blueprint dataset) (Supplementary Fig. 4a,b). These findings suggest a model where targeting a specific receptor on the cell surface may not be beneficial for patients. Instead, a distinct cell type expressing this molecule should be targeted (Fig. 4d). This can be achieved using various novel strategies in immunotherapy, such as the SynNotch system[45], which would allow targeting of a molecule on a particular cell type.

**Characterizing interacting cell types with single-cell resolution**

To validate these interactions, we used two independent published scRNA-Seq data sets[26,27], which interrogated the bone marrow immune microenvironment in relapsed/refractory multiple myeloma (RRMM) patients receiving IMiD-based treatments. We performed cell interaction analyses in these cohorts and assessed the overlap with our dataset (Fig. 5a). We identified a lower number of interactions in the scRNA-Seq datasets (Supplementary Fig. 5a) than in our low-input RNA-seq analyses, presumably related to the fact that a greater number of genes are detected in minipools than in single cells. Despite this and the fact that the validation datasets were from RRMM patients rather than newly diagnosed patients, the majority of predicted interactions identified overlapped with those derived from the low-input RNA-Seq (Fig. 5b,c). Most of the interactions were detected in all three datasets independently of interacting cell types (Fig. 5d). We further included an additional dataset of newly-diagnosed myeloma patients who went on to receive IMiD treatment[28] and found that the majority of predicted interactions identified overlapped with those derived from the low-input RNA-Seq (Supplementary Fig. 5b).

To investigate whether these interactions are IMiD-specific, we next investigated two datasets from patients that received non-IMiD-based treatments: GSE210079[29] for a BCMA-CAR-T treated patient population and GSE161801[27] consisting of patients, who received either MEKi or proteasome inhibitor treatment. We found that most of the detected interactions from the non-IMID based treatments overlap with our low-input RNA-Seq dataset, arguing that most interactions are not treatment-specific (Supplementary Fig. 5c-f). While most interactions were shared between datasets, regardless of treatment, this was not the case for the dual interactions. In fact, the dual interactions predicted from our low-input RNA-Seq dataset were not found as dual interactions in any of the other inspected datasets (IMiD- or non-IMiD-treated), arguing that these are specific to the dataset and the context (Supplementary Fig. 5g). However, discrepancies in the predicted number of interactions could affect the recovery of identical dual interactions.

To further delineate the immune compartments and pinpoint the specific cell types involved in interactions linked to favorable and unfavorable outcomes at the single-cell level, we leveraged a published single-cell dataset (GSE162337) profiling myeloma and immune cells from 9 relapsed/refractory multiple myeloma patients receiving Elo-PVD treatment[26]. Two interactions that were identified as dual interactions in both datasets are CD1D/LILRB2 and IL15/IL15RA. The interaction of IL15/IL15RA plays a role in adaptive and innate immunity and has been shown to be involved in myeloma progression[42,46]. Notably, in our low-input RNA-Seq dataset, TTPhigh patients showed an enriched IL15/IL15RA interaction specifically enriched between CD19+ cells interacting with CD3+ or CD45+TN cells, while in TTPlow patients the interaction was identified between CD19+ cells or between CD19+ and CD14+ cells (Fig. 4c). Similarly, in the scRNA-seq derived dataset[26], we identified the IL15/IL15RA interaction between CD19+ and CD3+ cells in the TTPhigh condition and were able to further define these cell types as naive B cells and CD8+ T cells. In the TTPlow patients, this same interaction was also found between CD19+ and CD14+ cells and we defined these as (class-switched) memory B cells or naive B cells and monocytes or macrophages, respectively (Fig. 5e).

Regarding CD1D/LILRB2, we detected an interaction between CD14+ and CD19+ cells in the TTPhigh patients and identified the interacting cell types as monocytes and memory B cells in the scRNA-Seq datasets. However, in the TTPlow patients, we recovered the same interaction between CD19+ and CD45+TN cells and identified memory B cells and eosinophils/neutrophils as the specific cell types driving this interaction (Fig. 5f). Therefore, by interrogating a distinct dataset with single-cell resolution, we were able to validate the ‘dual’ effect of candidate pathways, depending on the specific cell types involved. Lastly, to determine whether RNA expression could serve as a proxy for protein expression, we evaluated how RNA expression corresponded to protein expression in single cells measured by CITE-Seq for 49 different markers in a dataset assessing bone marrow myeloma and immune cells following BCMA CAR-T therapy[29]. We found that RNA levels generally reflected protein expression accurately

(Supplementary Fig. 6a,b), particularly for molecules well-established to define hematopoietic lineage and differentiation (Supplementary Fig. 6c-f).

## Discussion

Our study aimed to explore whether activating the same immune signaling pathway can yield different results. Our data imply that while activation of a pathway through interaction with one cell type can yield positive effects, its activation through interaction with another cell type can lead to negative effects.

We examined the immune microenvironments of newly diagnosed multiple myeloma patients who relapsed after IMiD-based therapy, since there is ample evidence for the interaction and the interdependence of MM cells and the immune microenvironment[27,47-51]. Using FACS sorting, low-input RNA-Seq, and computational deconvolution, we detected a shift from naive B cells to more differentiated memory B cells in patients with a worse prognosis, similar to changes we observed when comparing myeloma patients to normal donors. Our pathway enrichment analysis revealed that B cell differentiation-promoting interleukin signals, such as IL7, IL10, and IL15, and downstream JAK/STAT signaling, were enriched in the B cell compartment of poor-prognosis patients[52-56]. Our study therefore highlights the crucial role of the B cell compartment in response to IMiD-based therapy in newly diagnosed MM patients. These findings and the evolving understanding of B cell contributions to anti-tumor immunity were the reasons why we focused on the B cell compartment in this study.

In myeloma, long-term immunosurveillance is critical. Many immunotherapies stop working although the antigen is still expressed by the target cells, pointing to a dysfunctional immune response. Growing evidence indicates that T cell exhaustion due to prolonged antigen exposure

results in an immune system unable to efficiently combat tumors[57,58]. Lower tumor burdens and less immune activation may help maintain a more competent immune system, leading to a better prognosis. Our findings suggest that patients with good prognosis maintain a less differentiated B cell compartment, with naïve B cells and cytotoxic T and NK cells, while those with a poor prognosis exhibit a more differentiated B cell compartment that may promote a pro-inflammatory microenvironment.

Leveraging computational inference, we uncovered a complex network of cell-cell interactions within the immune system, pinpointing those that correlate with prognosis. Interestingly, some of these interactions are found in opposite prognostic conditions, conferring either favorable or poor prognosis depending on the specific cell types involved. Such signal ambiguity, as is known for IL2 signaling[59], which can promote T effector cells and immunosuppressive regulatory T cells at the same time, complicates these signals' characterization and targeting. Thus, understanding the cell types involved in these interactions can provide clearer insight into resistance mechanisms. For instance, we identified a dual role for the interaction of IL15/IL15RA. When IL15 expressed by B cells interacts with IL15RA on T or NK cells, it fosters a favorable prognosis, enhancing immune activation and cytotoxicity, and boosting CD8+ memory T cell efficacy[39-42]. Conversely, IL15 signaling involving CD14+ cells can promote pro-inflammatory cytokines and chemoattractants, such as IL1, IL6, IL8, TNF-α, and MCP-1[42-44], creating a pro-inflammatory immunosuppressive microenvironment. Thus, the outcome of the same interaction may vary based on the participating cell types.

These observations underscore the importance of considering specific cell types when targeting ligand-receptor interactions. Understanding this concept is of paramount importance for the development of more selective immunotherapies. Our findings advocate for a paradigm shift towards selectively targeting cells expressing specific molecules. While traditional

immunotherapy indiscriminately targets surface receptors, emerging technologies, like Chimeric antigen receptor T (CAR T) cells, permit cell-type-specific targeting of surface receptors[45]. This capability of conditional cellular therapies facilitates a more precise manipulation of the immune microenvironment and a promising avenue for optimizing therapeutic interventions, which allows for the specific targeting of detrimental immune signaling pathways while preserving essential immune functions and mitigating toxicities.

Given that cancer immunotherapies yield lasting responses in only a fraction of patients, there is a need for devising novel immunotherapeutic strategies. While T cells and NK cells have so far been the primary focus of immunotherapeutic interventions, recently it has been suggested that the manipulation of TIM-1 expressing B cells may facilitate the activation of the second arm of adaptive immunity, leading to improved anti-tumor immune responses[60]. Leveraging the diverse functions of B cells, including antigen presentation and production of antibodies, may open avenues for novel immunotherapeutic approaches, including combination therapies that exploit both T cell and B cell responses. Therefore, investigating the potential role of B cells is crucial for developing more comprehensive immunotherapeutic strategies. Further exploration of the interplay between B cells and other immune components within the tumor microenvironment therefore holds great promise for advancing the field of cancer immunotherapy.

In summary, our research demonstrates how diverse immune microenvironments in NDMM patients influence their responses to IMiDs and other therapies. We uncover the intricate signaling network within the bone marrow immune microenvironment, which critically impacts diverse immune cell functions. We further explain how different outcomes can result from the same molecular interaction, based on the participating cellular identities. Moving forward, selectively targeting cells expressing certain molecules, rather than just targeting the molecules

themselves, is crucial to balance beneficial and harmful signals, ensuring effective long-term tumor immunity.

**Acknowledgments**

Funding for this research was provided by Merck Sharp & Dohme LLC, a subsidiary of Merck & Co., Inc., Rahway, NJ, USA and the Multiple Myeloma Research Foundation (MMRF).

**Authorship Contributions**

J.F., P.A., T.V. and P.A. designed and performed data analysis. D.A. provided samples and advice, J.F., B.K. and J.G.L. designed experiments, provided project leadership, supervised the analysis, and wrote the manuscript. All authors discussed the results and reviewed the manuscript.

**Conflict of Interest Disclosures**

J.G.L. acknowledges the support of research funding for an unrelated project from Bristol Myers Squibb and the receipt of honoraria for consulting services provided to Asher Bio.

**References**

1 Dimopoulos, M. A. *et al.* Daratumumab, Lenalidomide, and Dexamethasone for Multiple Myeloma. *N Engl J Med* **375**, 1319-1331, doi:10.1056/NEJMoa1607751 (2016).

2 Dimopoulos, M. *et al.* Lenalidomide plus dexamethasone for relapsed or refractory multiple myeloma. *N Engl J Med* **357**, 2123-2132, doi:10.1056/NEJMoa070594 (2007).

3 Dimopoulos, M. *et al.* Response and progression-free survival according to planned treatment duration in patients with relapsed multiple myeloma treated with carfilzomib, lenalidomide, and dexamethasone (KRd) versus lenalidomide and dexamethasone (Rd) in the phase III ASPIRE study. *J Hematol Oncol* **11**, 49, doi:10.1186/s13045-018-0583-7 (2018).

4 Holstein, S. A. & McCarthy, P. L. Immunomodulatory Drugs in Multiple Myeloma: Mechanisms of Action and Clinical Experience. *Drugs* **77**, 505-520, doi:10.1007/s40265-017-0689-1 (2017).

5 Wang, S., Li, Z. & Gao, S. Key regulators of sensitivity to immunomodulatory drugs in cancer treatment. *Biomark Res* **9**, 43, doi:10.1186/s40364-021-00297-6 (2021).

6 Witzig, T. E. *et al.* Long-term analysis of phase II studies of single-agent lenalidomide in relapsed/refractory mantle cell lymphoma. *Am J Hematol* **92**, E575-E583, doi:10.1002/ajh.24854 (2017).
7 List, A. *et al.* Lenalidomide in the myelodysplastic syndrome with chromosome 5q deletion. *N Engl J Med* **355**, 1456-1465, doi:10.1056/NEJMoa061292 (2006).
8 Chanan-Khan, A. *et al.* Clinical efficacy of lenalidomide in patients with relapsed or refractory chronic lymphocytic leukemia: results of a phase II study. *J Clin Oncol* **24**, 5343-5349, doi:10.1200/JCO.2005.05.0401 (2006).
9 Xin, A. *et al.* A molecular threshold for effector CD8(+) T cell differentiation controlled by transcription factors Blimp-1 and T-bet. *Nat Immunol* **17**, 422-432, doi:10.1038/ni.3410 (2016).
10 Zavidij, O. *et al.* Single-cell RNA sequencing reveals compromised immune microenvironment in precursor stages of multiple myeloma. *Nat Cancer* **1**, 493-506, doi:10.1038/s43018-020-0053-3 (2020).
11 Garcia-Ortiz, A. *et al.* The Role of Tumor Microenvironment in Multiple Myeloma Development and Progression. *Cancers (Basel)* **13**, doi:10.3390/cancers13020217 (2021).
12 Ghobrial, I. M., Detappe, A., Anderson, K. C. & Steensma, D. P. The bone-marrow niche in MDS and MGUS: implications for AML and MM. *Nature Reviews Clinical Oncology*, doi:10.1038/nrclinonc.2017.197 (2018).
13 Noonan, K. *et al.* A novel role of IL-17-producing lymphocytes in mediating lytic bone disease in multiple myeloma. *Blood* **116**, 3554-3563, doi:10.1182/blood-2010-05-283895 (2010).
14 Picelli, S. *et al.* Full-length RNA-seq from single cells using Smart-seq2. *Nature protocols* **9**, 171-181, doi:10.1038/nprot.2014.006 (2014).
15 Dobin, A. *et al.* STAR: ultrafast universal RNA-seq aligner. *Bioinformatics* **29**, 15-21, doi:10.1093/bioinformatics/bts635 (2013).
16 Bolger, A. M., Lohse, M. & Usadel, B. Trimmomatic: a flexible trimmer for Illumina sequence data. *Bioinformatics* **30**, 2114-2120, doi:10.1093/bioinformatics/btu170 (2014).
17 Anders, S., Pyl, P. T. & Huber, W. HTSeq--a Python framework to work with high-throughput sequencing data. *Bioinformatics* **31**, 166-169, doi:10.1093/bioinformatics/btu638 (2015).
18 Li, B. & Dewey, C. N. RSEM: accurate transcript quantification from RNA-Seq data with or without a reference genome. *BMC Bioinformatics* **12**, 323, doi:10.1186/1471-2105-12-323 (2011).
19 McCarthy, D. J., Campbell, K. R., Lun, A. T. & Wills, Q. F. Scater: pre-processing, quality control, normalization and visualization of single-cell RNA-seq data in R. *Bioinformatics* **33**, 1179-1186, doi:10.1093/bioinformatics/btw777 (2017).
20 Lun, A. T., McCarthy, D. J. & Marioni, J. C. A step-by-step workflow for low-level analysis of single-cell RNA-seq data with Bioconductor. *F1000Res* **5**, 2122, doi:10.12688/f1000research.9501.2 (2016).
21 Schubert, M. *et al.* Perturbation-response genes reveal signaling footprints in cancer gene expression. *Nat Commun* **9**, 20, doi:10.1038/s41467-017-02391-6 (2018).
22 Newman, A. M. *et al.* Robust enumeration of cell subsets from tissue expression profiles. *Nat Methods* **12**, 453-457, doi:10.1038/nmeth.3337 (2015).
23 Efremova, M., Vento-Tormo, M., Teichmann, S. A. & Vento-Tormo, R. CellPhoneDB: inferring cell-cell communication from combined expression of multi-subunit ligand-receptor complexes. *Nat Protoc* **15**, 1484-1506, doi:10.1038/s41596-020-0292-x (2020).
24 Thul, P. J. & Lindskog, C. The human protein atlas: A spatial map of the human proteome. *Protein Sci* **27**, 233-244, doi:10.1002/pro.3307 (2018).

25 Bagger, F. O., Kinalis, S. & Rapin, N. BloodSpot: a database of healthy and malignant haematopoiesis updated with purified and single cell mRNA sequencing profiles. *Nucleic Acids Res* **47**, D881-D885, doi:10.1093/nar/gky1076 (2019).
26 Frede, J. *et al.* Dynamic transcriptional reprogramming leads to immunotherapeutic vulnerabilities in myeloma. *Nat Cell Biol* **23**, 1199-1211, doi:10.1038/s41556-021-00766-y (2021).
27 Tirier, S. M. *et al.* Subclone-specific microenvironmental impact and drug response in refractory multiple myeloma revealed by single-cell transcriptomics. *Nat Commun* **12**, 6960, doi:10.1038/s41467-021-26951-z (2021).
28 Yao, L. *et al.* Comprehensive Characterization of the Multiple Myeloma Immune Microenvironment Using Integrated scRNA-seq, CyTOF, and CITE-seq Analysis. *Cancer Res Commun* **2**, 1255-1265, doi:10.1158/2767-9764.CRC-22-0022 (2022).
29 Dhodapkar, K. M. *et al.* Changes in Bone Marrow Tumor and Immune Cells Correlate with Durability of Remissions Following BCMA CAR T Therapy in Myeloma. *Blood Cancer Discov* **3**, 490-501, doi:10.1158/2643-3230.BCD-22-0018 (2022).
30 Zheng, G. X. *et al.* Massively parallel digital transcriptional profiling of single cells. *Nat Commun* **8**, 14049, doi:10.1038/ncomms14049 (2017).
31 Hao, Y. *et al.* Integrated analysis of multimodal single-cell data. *Cell* **184**, 3573-3587 e3529, doi:10.1016/j.cell.2021.04.048 (2021).
32 Wu, X. *et al.* Altered T Follicular Helper Cell Subsets and Function in Chronic Lymphocytic Leukemia. *Front Oncol* **11**, 674492, doi:10.3389/fonc.2021.674492 (2021).
33 Yu, H. *et al.* Increased frequency of bone marrow T follicular helper cells in patients with immune-related pancytopenia. *Clin Dev Immunol* **2013**, 730450, doi:10.1155/2013/730450 (2013).
34 Yan, L. *et al.* T Follicular Helper Cells As a New Target for Immunosuppressive Therapies. *Front Immunol* **8**, 1510, doi:10.3389/fimmu.2017.01510 (2017).
35 Zhang, L. *et al.* Regulatory B cell-myeloma cell interaction confers immunosuppression and promotes their survival in the bone marrow milieu. *Blood Cancer J* **7**, e547, doi:10.1038/bcj.2017.24 (2017).
36 Yamamoto, L., Amodio, N., Gulla, A. & Anderson, K. C. Harnessing the Immune System Against Multiple Myeloma: Challenges and Opportunities. *Front Oncol* **10**, 606368, doi:10.3389/fonc.2020.606368 (2020).
37 Mendez-Ferrer, S. *et al.* Bone marrow niches in haematological malignancies. *Nat Rev Cancer* **20**, 285-298, doi:10.1038/s41568-020-0245-2 (2020).
38 Peinado, H. *et al.* Pre-metastatic niches: organ-specific homes for metastases. *Nat Rev Cancer* **17**, 302-317, doi:10.1038/nrc.2017.6 (2017).
39 Goldrath, A. W. *et al.* Cytokine requirements for acute and Basal homeostatic proliferation of naive and memory CD8+ T cells. *J Exp Med* **195**, 1515-1522, doi:10.1084/jem.20020033 (2002).
40 Kennedy, M. K. *et al.* Reversible defects in natural killer and memory CD8 T cell lineages in interleukin 15-deficient mice. *J Exp Med* **191**, 771-780, doi:10.1084/jem.191.5.771 (2000).
41 Lodolce, J. P. *et al.* IL-15 receptor maintains lymphoid homeostasis by supporting lymphocyte homing and proliferation. *Immunity* **9**, 669-676, doi:10.1016/s1074-7613(00)80664-0 (1998).
42 Perera, P. Y., Lichy, J. H., Waldmann, T. A. & Perera, L. P. The role of interleukin-15 in inflammation and immune responses to infection: implications for its therapeutic use. *Microbes Infect* **14**, 247-261, doi:10.1016/j.micinf.2011.10.006 (2012).
43 Alleva, D. G., Kaser, S. B., Monroy, M. A., Fenton, M. J. & Beller, D. I. IL-15 functions as a potent autocrine regulator of macrophage proinflammatory cytokine production:

608 evidence for differential receptor subunit utilization associated with stimulation or
609 inhibition. *J Immunol* **159**, 2941-2951 (1997).
610 44 Neely, G. G. *et al.* Monocyte surface-bound IL-15 can function as an activating receptor
611 and participate in reverse signaling. *J Immunol* **172**, 4225-4234,
612 doi:10.4049/jimmunol.172.7.4225 (2004).
613 45 Roybal, K. T. *et al.* Engineering T Cells with Customized Therapeutic Response
614 Programs Using Synthetic Notch Receptors. *Cell* **167**, 419-432 e416,
615 doi:10.1016/j.cell.2016.09.011 (2016).
616 46 Tinhofer, I., Marschitz, I., Henn, T., Egle, A. & Greil, R. Expression of functional
617 interleukin-15 receptor and autocrine production of interleukin-15 as mechanisms of
618 tumor propagation in multiple myeloma. *Blood* **95**, 610-618 (2000).
619 47 Lee, G. W. *et al.* The Derived Neutrophil-to-Lymphocyte Ratio Is an Independent
620 Prognostic Factor in Transplantation Ineligible Patients with Multiple Myeloma. *Acta*
621 *Haematol* **140**, 146-156, doi:10.1159/000490488 (2018).
622 48 Akhmetzyanova I, Aaron T, Galbo P, et al. Tissue-resident macrophages promote early
623 dissemination of multiple myeloma via IL-6 and TNFalpha. Blood Adv. 2021;5(18):3592-
624 3608. *Blood Adv* **6**, 4490, doi:10.1182/bloodadvances.2022007214 (2022).
625 49 Heider, U. *et al.* Novel aspects of osteoclast activation and osteoblast inhibition in
626 myeloma bone disease. *Biochem Biophys Res Commun* **338**, 687-693,
627 doi:10.1016/j.bbrc.2005.09.146 (2005).
628 50 Musolino, C. *et al.* Inflammatory and Anti-Inflammatory Equilibrium, Proliferative and
629 Antiproliferative Balance: The Role of Cytokines in Multiple Myeloma. *Mediators Inflamm*
630 **2017**, 1852517, doi:10.1155/2017/1852517 (2017).
631 51 Tsirakis, G. *et al.* Clinical significance of interleukin-22 in multiple myeloma. *Hematology*
632 **20**, 143-147, doi:10.1179/1607845414Y.0000000182 (2015).
633 52 Heine, G. *et al.* Autocrine IL-10 promotes human B-cell differentiation into IgM- or IgG-
634 secreting plasmablasts. *Eur J Immunol* **44**, 1615-1621, doi:10.1002/eji.201343822
635 (2014).
636 53 Hiroi, T., Yanagita, M., Ohta, N., Sakaue, G. & Kiyono, H. IL-15 and IL-15 receptor
637 selectively regulate differentiation of common mucosal immune system-independent B-1
638 cells for IgA responses. *J Immunol* **165**, 4329-4337, doi:10.4049/jimmunol.165.8.4329
639 (2000).
640 54 Benito-Miguel, M. *et al.* IL-15 expression on RA synovial fibroblasts promotes B cell
641 survival. *PLoS One* **7**, e40620, doi:10.1371/journal.pone.0040620 (2012).
642 55 Armitage, R. J., Macduff, B. M., Eisenman, J., Paxton, R. & Grabstein, K. H. IL-15 has
643 stimulatory activity for the induction of B cell proliferation and differentiation. *J Immunol*
644 **154**, 483-490 (1995).
645 56 Corfe, S. A. & Paige, C. J. The many roles of IL-7 in B cell development; mediator of
646 survival, proliferation and differentiation. *Semin Immunol* **24**, 198-208,
647 doi:10.1016/j.smim.2012.02.001 (2012).
648 57 Zelle-Rieser, C. *et al.* 1T cells in multiple myeloma display features of exhaustion and
649 senescence at the tumor site. *Journal of Hematology and Oncology* **9**, 1-12,
650 doi:10.1186/s13045-016-0345-3 (2016).
651 58 Cohen, A. D. *et al.* How to Train Your T Cells: Overcoming Immune Dysfunction in
652 Multiple Myeloma. *Clin Cancer Res* **26**, 1541-1554, doi:10.1158/1078-0432.CCR-19-
653 2111 (2020).
654 59 Knoechel, B., Lohr, J., Kahn, E., Bluestone, J. A. & Abbas, A. K. Sequential
655 development of interleukin 2-dependent effector and regulatory T cells in response to
656 endogenous systemic antigen. *J Exp Med* **202**, 1375-1386, doi:10.1084/jem.20050855
657 (2005).

60 Bod, L. *et al.* B-cell-specific checkpoint molecules that regulate anti-tumour immunity. *Nature* **619**, 348-356, doi:10.1038/s41586-023-06231-0 (2023).

## Figure legends

**Figure 1. Characterization of bone marrow immune environment in treatment-naive MM patients.**

**a,b)** Patient characteristics. **a)** Time to progression for n=25 patients with data available (median=28 months, range 0-72 months). **b)** Treatment data for patients included in this study. Shown is percentage of patients who received a first line treatment including an IMiD. **c)** Diagram showing sorting strategy. **d)** Flow percentages for individual cell populations. Patients are ordered by time to progression (TTP). **e)** Patients with early (TTPlow) and late (TTPhigh) relapse were divided by median TTP. **f)** Bar plot showing flow percentages for individual populations comparing TTPlow vs TTPhigh patients. Significance was assessed using an unpaired t-test; * $p \leq 0.05$. **g)** Dot plots showing the distribution of values for individual cell populations shown in **f)**. Significance was assessed using an unpaired t-test; * $p \leq 0.05$. **h)** Experimental workflow. Low-input RNA-sequencing of 100-cell pools was performed using the Smart-Seq2 protocol. **i)** Tsne plot showing samples colored by sort marker. **j**) Expression of canonical marker genes for individual cell types across immune cell subsets.

**Figure 2. Differential enrichment of B-cell subsets associated with prognosis**

**a)** Analysis of the cell types composing the flow-sorted CD3+, CD14+, CD19+ and CD45+TN immune compartments according to gene signatures from Azimuth[31]. ASDC, AXL+ Dendritic Cell; BaEoMa, basophil eosinophil mast progenitor; cDC1, CD141+ myeloid dendritic cell; cDC2, CD1c+ myeloid dendritic cell; CD8 effector.1, memory-like CD8+GZMK+ alpha-beta T cell; CD8 effector.2, late differentiated CD8+GZMB+ cytotoxic alpha-beta T cell; CD8 effector.3, NKT-like CD8+ alpha-beta T cell; ILC, innate lymphoid cell; MAIT, mucosal associated invariant T; Mono, monocyte; NKdim, CD56dim NK cell; NKbright, CD56bright NK cell. **b)** Experimental workflow. Low-input RNA-sequencing was performed of individual cell populations sorted based on indicated markers from the bone marrow of 25 newly diagnosed myeloma patients (NDMM).

687 Cibersort was used to deconvolute cell type composition. **c-f)** Bar graphs showing the
688 composition of individual immune cell compartments based on deconvolution in NDMM patients.
689 Shown are percentages of cell types inferred by cibersort for CD19+ cells (**c**), CD3+ cells (**d**),
690 CD45posTN cells (**e**) and CD14+ cells (**f**). **g**) Patients with early (TTPlow) and late (TTPhigh)
691 relapse were divided by median TTP. **h**) Heatmap showing relative differences in cell type
692 abundance between patients with poor vs good prognosis. **i-l**) Dot plots showing the distribution
693 of values for the indicated cell populations comparing TTPlow with TTPhigh. Significance was
694 assessed using an unpaired t-test; * $p \leq 0.05$. **k**) Log2 ratio of naive/memory B cells in TTPlow
695 vs TTPhigh patients. Significance was assessed using an unpaired t-test; * $p \leq 0.05$. **m**)
696 Relative scores for a gene set for naive B cells in TTPlow vs TTPhigh patients.* $p \leq 0.05$ by
697 unpaired t-test. Bottom: Correlation of relative scores for naive B cell gene set vs TTP value.
698 R=0.56, p = 0.036. **n**) Expression of canonical marker genes for naive and memory B cells in
699 TTPlow vs TTPhigh patients. **o**) Expression of marker genes distinguishing B cells in TTPlow
700 and TTPhigh patients. **p**) Heatmap comparing activity of signaling pathways between TTPlow vs
701 TTPhigh patients.
702
703 **Figure 3. Association of the B-cell interactome with MM progression.**
704 **a**) Diagram. Interactions were determined using CellPhoneDB for patients with early or late
705 relapse. **b**) Comparison of the number of CellPhoneDB-predicted interactions between TTPlow
706 and TTPhigh samples. **c**) Diagram illustrating B-cell-centric interactions where B cells interact
707 with various other cell types. **d**) Heatmap comparing the interactome of B cells with other cell
708 types in TTPlow vs TTPhigh patients. **e**) Number of prognostic interactions vs total interactions
709 by condition.
710
711 **Figure 4. Dual interactions in B cells.**

**a**) Model of dual interactions. Left: Model of “Cellular-partner selectivity”. Given molecule A and molecule B (undefined ligand-receptor interacting pair), B cells (illustrated as CD19, grey) express exclusively molecule A on the cell surface and the other cells in their vicinity present molecule B. Prognosis is based on the engaged cell type. Right: Model based on “directionality” of the signaling. Given molecule A and molecule B (undefined ligand-receptor interacting pair), the B cell (illustrated as CD19, grey) presents both ligand and receptor molecules. Prognosis is determined by the directionality of the signal upon binding of the complementary molecule, which is expressed by other cells in the surroundings. **b**) Proportion of dual interactions established between each possible immune pair under study and their distribution in each prognostic condition. **c**) Heatmap showing dual interactions with potential targetability in MM. Displayed are the percentage of cells expressing the molecule and the median expression of both molecules by the pair of engaged cell types. Highlighted are those interactions which are significant ($p<0.05$) in one condition, but not the other. In the shown interactions, the first molecule is expressed in all cases by CD19+ cells (B cells); the second molecule is expressed by the four cell types (CD3+, CD14+, CD19+ or CD45+TN). On the left side of the list of interactions, the column represents TTPlow patients; on the right side, the column represents TTPhigh patients. **d**) Model illustrating IL15 – IL15RA interactions on diverse cell types as example.

**Figure 5. Validation of prognostically relevant cell-cell interactions in independent single-cell sequencing cohorts.**

**a)** Diagram. **b-d**) Venn diagrams showing overlap between interactions identified in TTPlow/TTPhigh patients of our cohort with published cohorts utilizing single-cell RNA-Seq. **e,f**) Examples of dual interactions that were detected with statistically significance in our cohort and published cohorts utilizing single-cell RNA-Seq. CS Memory B cells = class-switched memory B cells.

738

739 **Visual abstract**

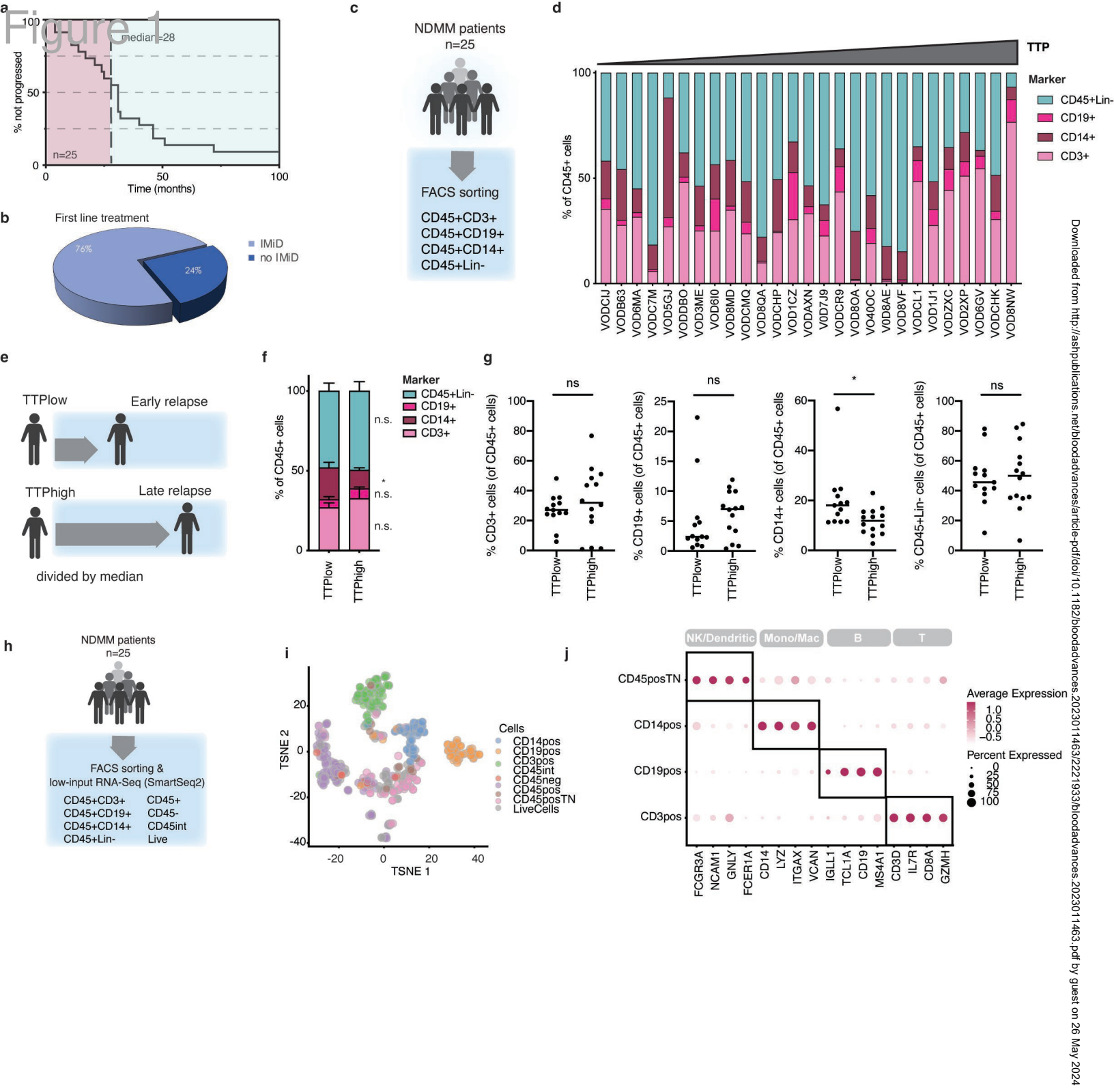




**Figure 1**

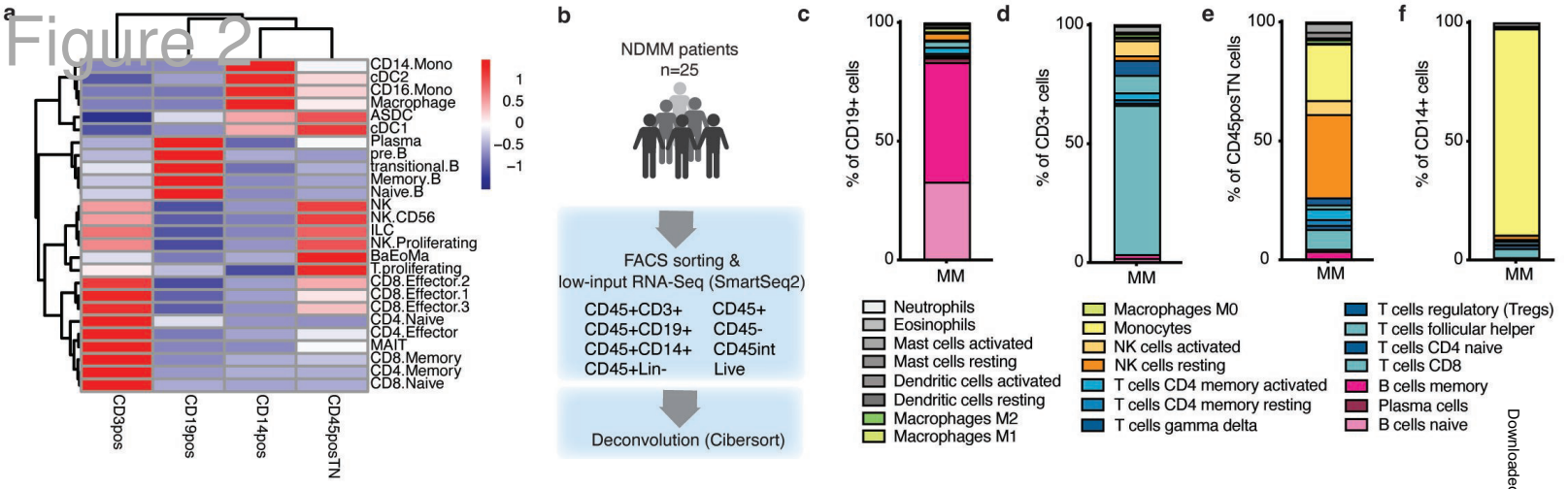


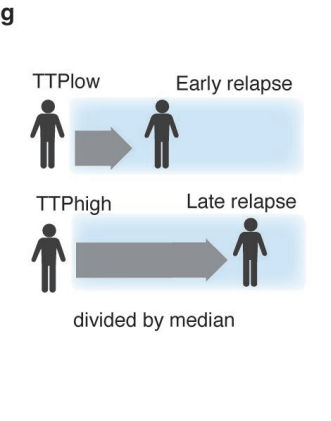


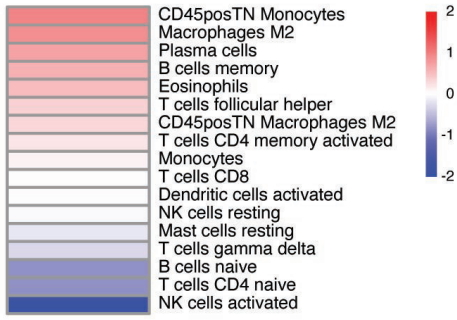


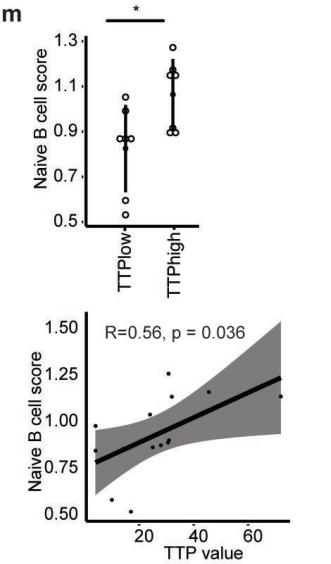


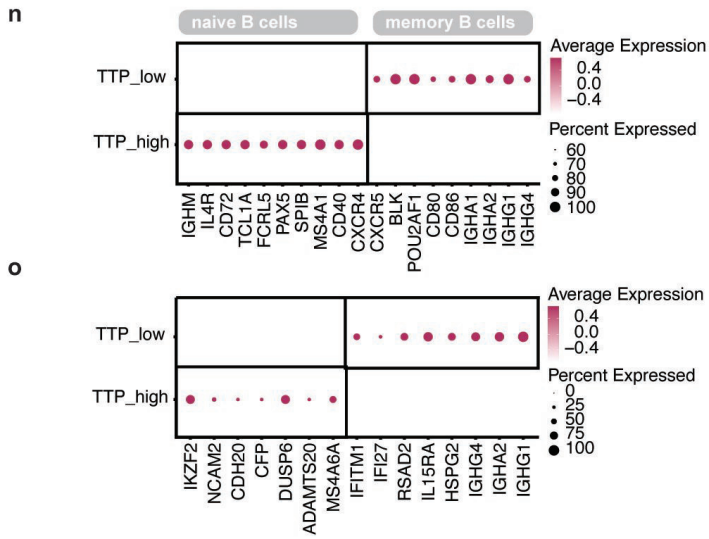








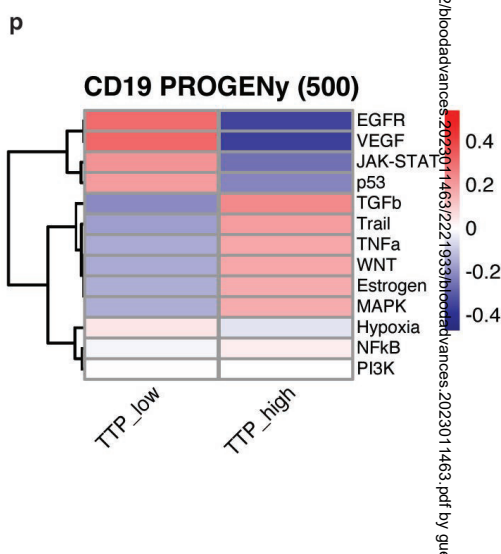




**Figure 2**

# Figure 3

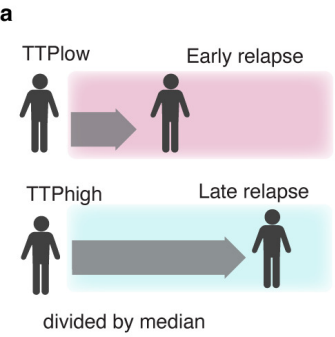


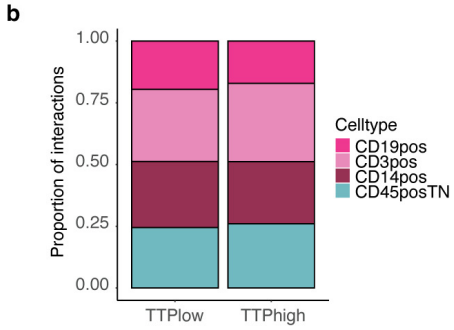


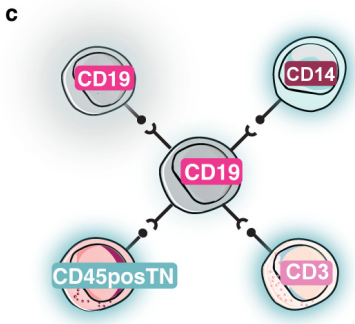


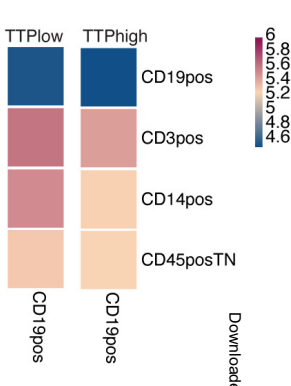


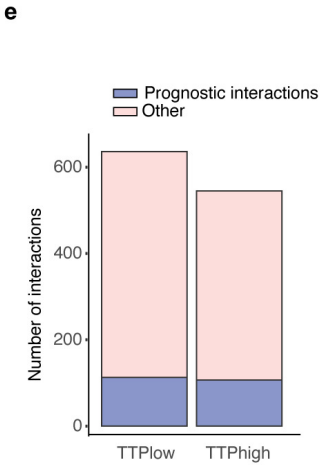




**Figure 3**

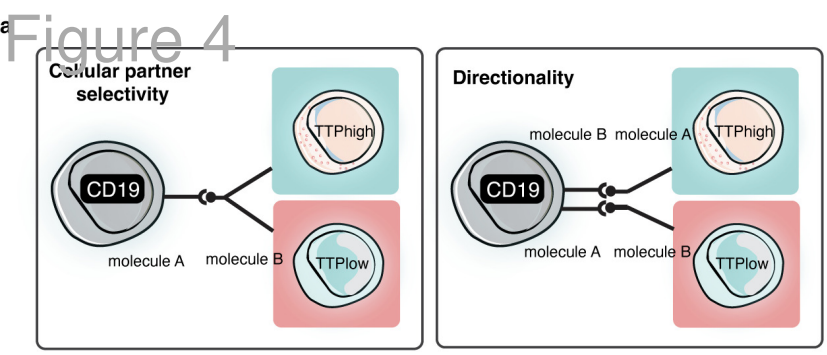


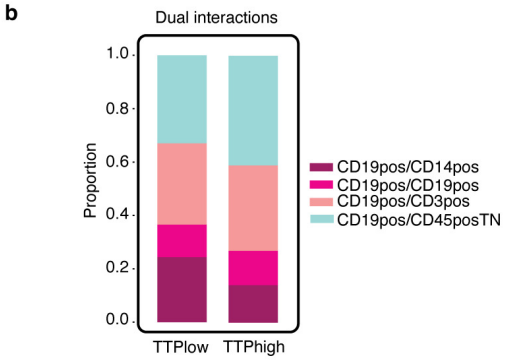


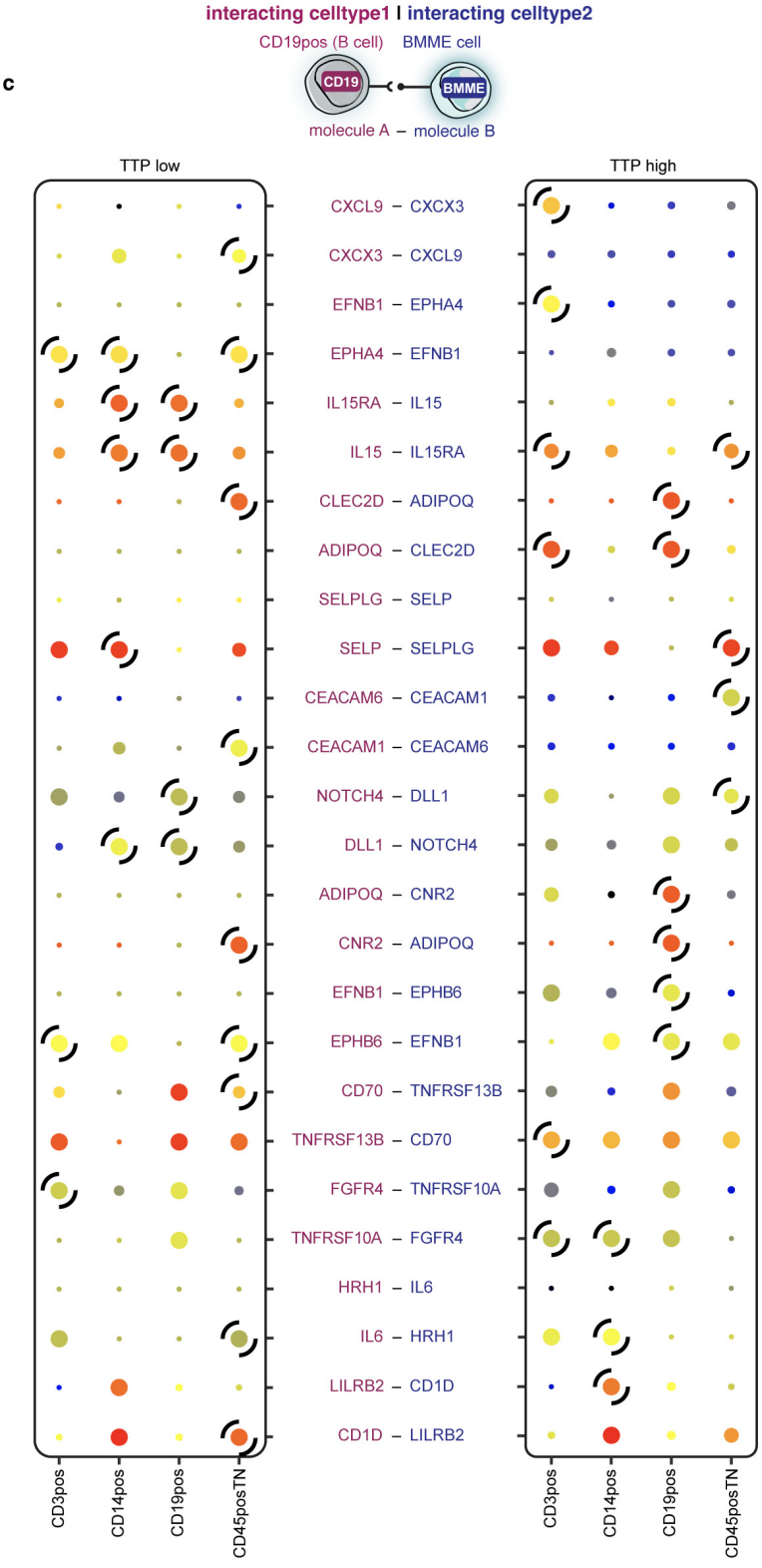


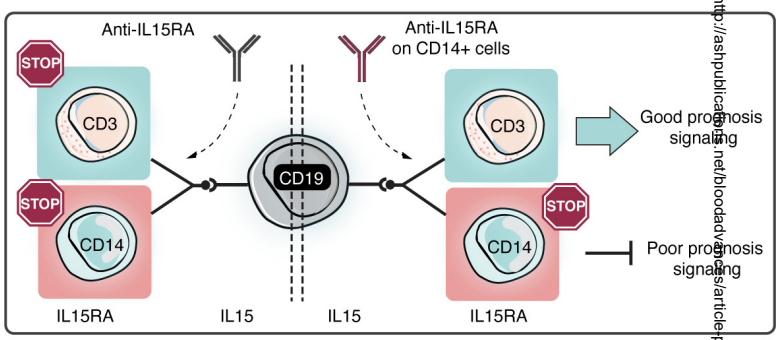


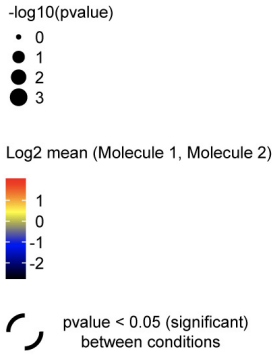




Figure 4

# Figure 5

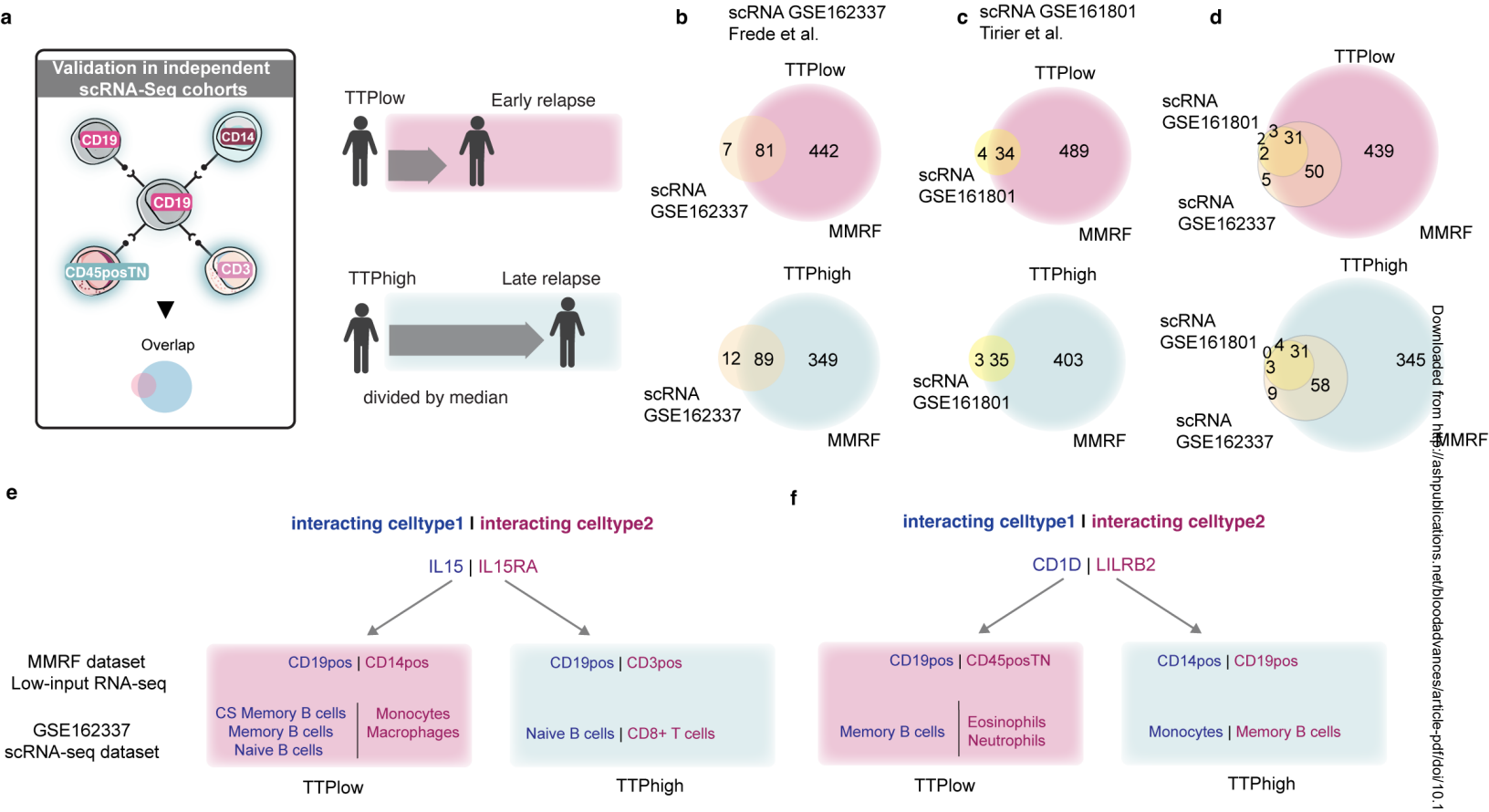







**Figure 5**